BARF1 gene silencing triggers caspase-dependent mitochondrial apoptosis in Epstein-Barr virus-positive malignant cells

TAZNIM BEGAM MOHD MOHIDIN and CHING CHING NG*

Institute of Biological Sciences (Genetics and Molecular Biology), Faculty of Science, University of Malaya, Kuala Lumpur, Malaysia

**Corresponding author (Email, ccng@um.edu.my)*

Epstein-Barr virus (EBV)-encoded BARF1 (BamH1-A Rightward Frame-1) is expressed in EBV-positive malignancies such as nasopharyngeal carcinoma, EBV-associated gastric cancer, B-cell lymphoma and nasal NK/T-cell lymphoma, and has been shown to have an important role in oncogenesis. However, the mechanism by which BARF1 elicits its biological effects is unclear. We investigated the effects of BARF1 silencing on cell proliferation and apoptosis in EBV-positive malignant cells. We observed that BARF1 silencing significantly inhibits cell proliferation and induces apoptosis-mediated cell death by collapsing the mitochondrial membrane potential in AG876 and Hone-Akata cells. BARF1 knockdown up-regulates the expression of pro-apoptotic proteins and down-regulates the expression of anti-apoptotic proteins. In BARF1-down-regulated cells, the Bcl-2/BAX ratio is decreased. The caspase inhibitor z-VAD-fmk was found to rescue siBARF1-induced apoptosis in these cells. Immunoblot analysis showed significant increased levels of cleaved caspase 3 and caspase 9. We observed a significant increase in cytochrome c level as well as the formation of apoptosome complex in BARF1-silenced cells. In conclusion, siRNA-mediated BARF1 down-regulation induces caspase-dependent apoptosis via the mitochondrial pathway through modulation of Bcl-2/BAX ratio in AG876 and Hone-Akata cells. Targeting BARF1 using siRNA has the potential to be developed as a novel therapeutic strategy in the treatment of EBV-associated malignancies.

[Mohidin TBM and Ng CC 2015 BARF1 gene silencing triggers caspase-dependent mitochondrial apoptosis in Epstein-Barr virus-positive malignant cells. *J. Biosci.* **40** 41–51] **DOI** 10.1007/s12038-015-9502-z

1. Introduction

Epstein-Barr virus (EBV) has been intensively studied over the past years due to its association with a number of cancers. EBV encodes the oncogene LMP1 (Latent Membrane Protein-1) and a candidate oncogene BARF1 (BamH1-A Rightward Frame-1). LMP1 and BARF1 play important roles in cellular gene expression and are thought to be involved in EBV-mediated tumorigenesis (Wei and Ooka 1989; Wei *et al*. 1997). Interestingly, BARF1 was expressed in the absence of LMP1 or lytic proteins in primary primate kidney epithelial cells immortalized by EBV infection (Danve *et al*. 2001). BARF1 expression has been detected in malignant epithelial cells and also in B cells. BARF1 expression was demonstrated in Malawian B-lymphoma (Xue *et al*. 2002) and in nasal NK/T-cell lymphoma (Zhang *et al*. 2006). BARF1 is also expressed at high levels consistently in nasopharyngeal carcinoma (NPC) (Decaussin *et al*. 2000; Seto *et al.* 2005), in EBV-associated gastric carcinoma (GC) (Zur Hausen *et al*. 2000) and in EBV-immortalized epithelial cells (Danve *et al*. 2001).

When expressed endogenously, BARF1 is secreted from cells (Sall *et al*. 2004; de Turenne-Tessier *et al*. 2005; Fiorini and Ooka, 2008; Seto *et al*. 2008). BARF1 is known to

Keywords. Apoptosis; cancer; caspase; EBV; mitochondria

Supplementary materials pertaining to this article are available on the *Journal of Biosciences* Website at *http://www.ias.ac.in/jbiosci/mar2015/supp/Mohidin.pdf*

Published online: 4 February 2015

induce a malignant transformation in established rodent fibroblasts (Wei and Ooka 1989), primary primate epithelial cells (Wei *et al*. 1997) and in human EBV-negative B cells (Sheng *et al*. 2001). The introduction of recombinant EBV carrying the BARF1 gene into EBV-negative cell lines did not alter the expression level of bcl-2 but induced NPC cell tumorigenicity in nude mice (Seto *et al*. 2008). Introduction of BARF1 into primary primate kidney epithelial PATAS cells led to morphological changes as well as continuous cell growth (Wei *et al*. 1997). BARF1 together with H-Ras was reported to be able to transform human epithelial cells (Jiang *et al*. 2009). Purified BARF1 from serum showed a powerful mitogenic activity (Houali *et al*. 2007). BARF1 is also recognized by NK cells in ADCC (antibody-dependent cellular cytotoxicity) test (Tanner *et al*. 1997). Hence, BARF1 may be involved in oncogenic mechanism and also in immunomodulation.

BARF1 has been shown to activate the anti-apoptotic protein Bcl-2 in rodent fibroblasts (Sheng *et al*. 2001) and in EBV-negative human Akata B cells transfected by BARF1 (Sheng *et al*. 2003), suggesting an anti-apoptotic role of BARF1. Furthermore, BARF1 expression in gastric cancer cells protected the cells from apoptosis through an increased Bcl-2 to BAX ratio (Wang *et al*. 2006). Collectively, these findings indicate that besides promoting cell proliferation, BARF1 may function as a survival factor by suppressing apoptosis pathway. However, the exact mechanism of how the anti-apoptotic effect of BARF1 is mediated remains to be clarified. Hence, in this study we aimed to investigate the molecular mechanisms by which BARF1 employs in its anti-apoptotic function.

2. Materials and methods

2.1 *Cell culture conditions*

AG876 (obtained from American Type Culture Collection, USA) and Hone-Akata (a gift from Prof Sam Choon Kook) (Glaser *et al*. 1989) were used in this study. AG876 and Hone-Akata cells were grown in RPMI-1640 medium (GIBCO/BRL, USA) supplemented with 1% penicillin/streptomycin (GIBCO/BRL, USA) and 10% (v/v) fetal bovine serum (GIBCO/BRL, USA) at 37°C under a humidified atmosphere of 95% air and 5% CO_2. Cells were passaged upon reaching 80% confluence.

2.2 *siRNA synthesis*

siRNAs were synthesized and purified by Ambion Inc. (USA). We designed three siRNAs against the different positions of BARF1 open reading frame (189-207, 409-427, and 545-563; GenBank accession no. V01555) using Ambion's online siRNA finder (*http://www.ambion.com/techlib/misc/siRNA_finder.html*). The three siRNAs were tested for the most effective gene knockdown ability. siRNA targeting the position 409-427 reduced the BARF1 mRNA level most significantly compared with the other two siRNAs. Hence, this siRNA termed siBARF1 was selected for subsequent experiments. The siBARF1 sequence is sense: 5′-CCAGACUUCUCUGUCCUUAtt-3′ and antisense: 5′-UAAGGACAGAGAAGUCUGGga-3′. A negative control siRNA (siNEG) which had no significant homology to any coding sequences in human and EBV genome was also synthesized and used.

2.3 *siRNA transfection*

The reverse transfection method was employed to deliver siRNA molecules into cell lines. In the reverse transfection method, cells are in suspension compared to the traditional pre-plating method. As the cells are in suspension, a larger amount of cell surface is exposed to transfection agent/siRNA complexes, thus contributing to the improved transfection efficiency. siRNAs were transfected into the cells using siPORT *NeoFX* (Ambion Inc., USA) transfection agent using the double transfection method. Briefly, siRNA was diluted to 35 nM in 100 µL Opti-MEM I medium and 5 µL of siPORT *NeoFX* was diluted in 100 µL Opti-MEM I medium. Diluted siRNA and diluted transfection agent were mixed gently, incubated at room temperature for 10 min and dispensed into the culture plate. Cell suspensions were overlaid onto the transfection complexes in six-well plates at a density of 2.4×10^5 cells/well. Plates were rocked gently to ensure proper distribution of transfection complexes to the cells and incubated for 24 h. We performed a re-transfection of adherent cells with 35 nM siBARF1 the following day.

2.4 *RNA extraction and reverse transcription PCR (RT-PCR)*

Total RNA was extracted from cells using the RNeasy Mini Kit® (Qiagen, Germany) according to the manufacturer's protocol. RNA was subjected to DNase (Invitrogen, USA) treatment and then used as a template for reverse transcription. For first strand cDNA synthesis, SuperScript™ III First-Strand Synthesis System (Invitrogen, USA) was used. Equal amounts of cDNA were subjected to PCR analysis. For qPCR analysis, real-time PCR runs were performed using Rotor-Gene™ 6000 (Qiagen, Germany). Each reaction contained 1× TaqMan® Universal PCR Master Mix, No AmpErase® UNG (Applied Biosystems), 1× BARF1 primers and TaqMan® probes mix and cDNA in a final volume of 20 µL. Cycling conditions were as follows: 10 min at 95 °C followed by 40 cycles of 15 s at 95°C and

1 min at 60°C. For semi-quantitative PCR, gene-specific primers with the concentration of 10 μM were used in a total reaction volume of 50 μL. The sequences of the primers were: Bcl-2 forward: 5′-CCTGTGGATGACTGAGTACC-3′ and reverse: 5′-GAGACAGCCAGGAGAAATCA-3′, BAX forward: 5′-GTTTCATCCAGGATCGAGCAG-3′ and reverse: 5′-CATCTTCTTCCAGATGGTGA-3′, GAPDH forward: 5′-TGCCTCCTGCACCACCAACT-3′ and reverse: 5′-CGCCTGCTTCACCACCTTC-3′. The amplification conditions were 30 cycles at 94°C for 30 s, 53°C for 30 s, and 72°C for 30 s. Amplified products were analysed by agarose gel electrophoresis. Data were analysed with ImageJ software and expression levels of Bcl-2 and BAX were normalized to GAPDH.

2.5 *Trypan blue exclusion assay*

Cell pellet was re-suspended thoroughly in 1 mL of 1× PBS to disperse any clumps. A 50 μL cell suspension was added to 450 μL of 0.4% trypan blue in a microcentrifuge tube and mixed gently. Then, 10 μL of cell suspension was transferred immediately to the edge of a hemocytometer (Improved Neubauer) chamber. The slide was then transferred to the microscope stage and cells lying within the 1 mm^2 area in the central area of the grid were counted manually using a tally counter. The concentration of cells was calculated using the following formula: $c = n \times$ dilution factor $\times 10^4$, where c is the cell concentration (cells/ml) and n is the number of cells counted.

2.6 *WST-1 (water-soluble tetrazolium salt) assay*

Cells were seeded in microplates (tissue culture grade, 96 wells, flat bottom) in 0.1 mL of 10% fetal bovine serum (FBS)-supplemented RPMI-1640 medium at a concentration of 4×10^3 cells/well. Cells were incubated for 48 , 72 and 96 h at 37°C with 5% CO_2. For each incubation time, different plates were used. On the day of the assay, 10 μL/well of Cell Proliferation Reagent WST-1 (Roche, Germany) was added and incubated for 4 h at 37°C and 5% CO_2. Plates were shaken thoroughly for 1 min on a shaker. The optical density (OD) of the samples was measured at 450 nm against a background control as blank using a microplate (ELISA) reader. The experiments were repeated at least three times, independently, to verify the reproducibility of the results.

2.7 *Annexin V staining*

Cells were stained using Annexin V-FITC kit (Miltenyi Biotec, Germany) according to manufacturer's protocols. Briefly, 10^6 cells were washed with 1× Binding Buffer and centrifuged at 300*g* for 10 min. Cell pellet was resuspended in 100 μL of 1× Binding Buffer. Then, 10 μL of Annexin V-FITC per 10^6 cells was added, mixed well and incubated for 15 min in the dark at room temperature. Cells were washed by adding 1 mL of 1× Binding Buffer per 10^6 cells and centrifuged at 300*g* for 10 min. Cell pellet was resuspended in 500 μl of 1× Binding Buffer and 5 μl of PI solution was added immediately prior to analysis by Miltenyi MacsQuant flow cytometer.

2.8 *Western blotting*

Cells were harvested and rinsed with PBS. Total cellular protein was extracted using M-PER Mammalian Protein Extraction Reagent (Thermo-Scientific, USA) according to the manufacturer's protocols. For extraction of mitochondria and cytosolic fractions, we used the Mitochondria Isolation Kit for cultured cells (Thermo-Scientific, USA) according to the manufacturer's protocols. Culture media was collected and centrifuged at 3000*g* for 10 min to eliminate cellular debris. Following clearing, 10 ml culture media were concentrated to 10 μL with Vivaspin 15R centrifugal filter (Vivascience, Inc). Examination of secreted BARF1 expression was performed using this concentrated fraction. Equal amount of protein (40 μg) from each sample was subjected to 10% SDS-PAGE and transferred onto PVDF membranes (Millipore, USA). After blocking with 1% blocking solution (KPL, USA) for 2 h at room temperature, membranes were incubated with primary antibodies overnight at 4°C. Antibodies against Bcl-2, BAX, PARP, caspase 9, caspase 3, cytochrome c, CoxIV and Apaf-1 were obtained from Cell Signaling Technology (USA), anti-GAPDH was obtained from Abnova (USA) and anti-β-actin was obtained from Abcam (USA). BARF1 antibody (MoAb 4A6) was kindly provided by Dr. Middeldorp (Seto *et al*. 2005; de Turenne-Tessier *et al*. 2005; Hoebe *et al*. 2011, 2012a, b; Chang *et al*. 2013). The membranes were then incubated with AP-conjugated or HRP-conjugated secondary antibody raised against the respective species for 1 h at room temperature. Blots probed with AP-conjugated antibodies were developed with NBT/BCIP substrate (KPL, USA) and signals from HRP-conjugated antibodies were developed using LumiGLO reagent (Cell Signalling Technology, USA) and imaged with Biospectrum 415, UVP. Quantification of bands using densitometry analysis was performed using ImageJ software.

2.9 *Mitochondrial membrane potential (MMP)*

Evaluation of changes in mitochondrial membrane potential (MMP) in cells was carried out using the APO LOGIX JC-1 Mitochondrial Membrane Potential Assay Kit (Cell Technology Inc, USA) according to the manufacturer's

instructions. Briefly, about 0.5 ml cell suspension was centrifuged for 5 min at room temperature at 400*g*. Cell pellet was resuspended in 0.5 mL 1× JC-1 reagent. Cells were then incubated at 37°C in a 5% CO_2 incubator for 15 min. This was followed by centrifugation for 5 min at 400*g*. The cell pellet was resuspended in 2 mL 1× Assay Buffer, centrifuged and supernatant was removed. Cell pellet was resuspended in 0.5 mL 1× Assay Buffer and analysed immediately using Miltenyi MacsQuant flow cytometer. Mitochondria containing red JC-1 aggregates in healthy cells are detectable in the FL2 channel and green JC-1 monomers in apoptotic cells are detectable in the FITC channel (FL1).

2.10 *Apoptosis antibody array*

Detection of apoptotic proteins was done using the RayBio® Human Apoptosis Antibody Array kit with the glass-slide array format AAH-APO-G1 (RayBioTech, USA). This kit detects 43 different apoptotic proteins as well as GAPDH (Glyceraldehyde 3 phosphate dehydrogenase) as a loading control indicator for protein samples with picogram-per-milliliter (pg/mL) sensitivity. The array slide was scanned with G2505C microarray scanner (Agilent Technologies) using the cy3 (green) channel. The image extraction and data analyses were done using GenePix® Pro Microarray Acquisition and Analysis software version 6.1.0.4 (Agilent Technologies). The background corrected raw intensity values were used for analysis. The biotin-conjugated proteins produce fluorescence signals, which were used to identify the orientation and to compare the relative expression levels among the different wells. The positive controls are biotinylated antibody. Standardized amounts of biotinylated IgG are printed directly onto each array and if all other variables are the same, the positive control intensities will be equal. The positive controls monitor the detection process and were used for normalization. Background corrections and normalization were done using the RayBio antibody array analysis tool.

2.11 *Immunoprecipitation*

We immunoprecipitated caspase 9 from 400 µg of total protein with anti-caspase 9 antibody (Cell Signaling Technology, USA) and 20 µL of protein A agarose beads (Santa Cruz Biotechnology, USA). Precipitates were washed five times with M-PER Mammalian Protein Extraction Reagent (Thermo-Scientific, USA) and once with PBS. The pellet was resuspended in 1× sample buffer [50 mM Tris (pH 6.8), 100 mM bromophenol blue and 10% glycerol]. This solution was incubated at 90°C for 10 min, electrophoresed and immunoblotted with anti-Apaf-1 (Cell Signaling Technology, USA).

3. Results

3.1 *BARF1 siRNA suppresses the expression of BARF1*

To investigate the molecular mechanisms of BARF1 with regards to cell proliferation and apoptosis, the expression of this gene was knocked down using siRNA (siBARF1) in AG876 and Hone-Akata cells. To assess the efficiency of BARF1 silencing, total RNA from siRNA-treated and control cells was isolated. After cDNA synthesis, quantitative real-time (qRT)-PCR (Taqman) targeting BARF1-specific sequence was used to determine BARF1 mRNA expression levels. Results were expressed in absolute terms as the number of copies of BARF1 gene. In AG876 and Hone-Akata cells, transfection with siBARF1 suppressed BARF1 expression to 10% and 15% residual levels 48 h post transfection whereas no significant difference in knockdown efficiency was observed using siNEG when compared with untreated control (figure 1A). To substantiate the qRT-PCR data, we performed immunoblotting using anti-BARF1 monoclonal antibody to detect the BARF1 protein expression in both culture medium as well as cell lysate. Western blot analysis of cell lysate showed a reduction in BARF1 protein band intensity in both cell lines that were treated with siBARF1 when compared with siNEG and untreated controls (figure 1B). However, our attempts to detect the secreted form of BARF1 protein from the concentrated culture media using Western blot failed (data not shown). We have also confirmed BARF1 mRNA and protein expression down-regulation using another siRNA (siBARF1-2) targeting position 545-563 of BARF1 open reading frame (supplementary figure 1A–B).

3.2 *Silencing of BARF1 expression inhibits cell proliferation*

The effect of BARF1 depletion on the viability of AG876 and Hone-Akata cells was determined by the trypan blue exclusion test. As shown in figure 1C, the number of control cells (untreated and siNEG-treated) continued to increase in a time-dependent manner. However, cell proliferation was significantly inhibited 72 h post-transfection in BARF1-depleted cells when compared with the controls. To confirm the effect of BARF1 knockdown on cell proliferation, we used the WST-1 cell proliferation assay. Our results indicated that at 72 h post-transfection, the growth of siBARF1-transfected cells was inhibited substantially in both AG876 and Hone-Akata

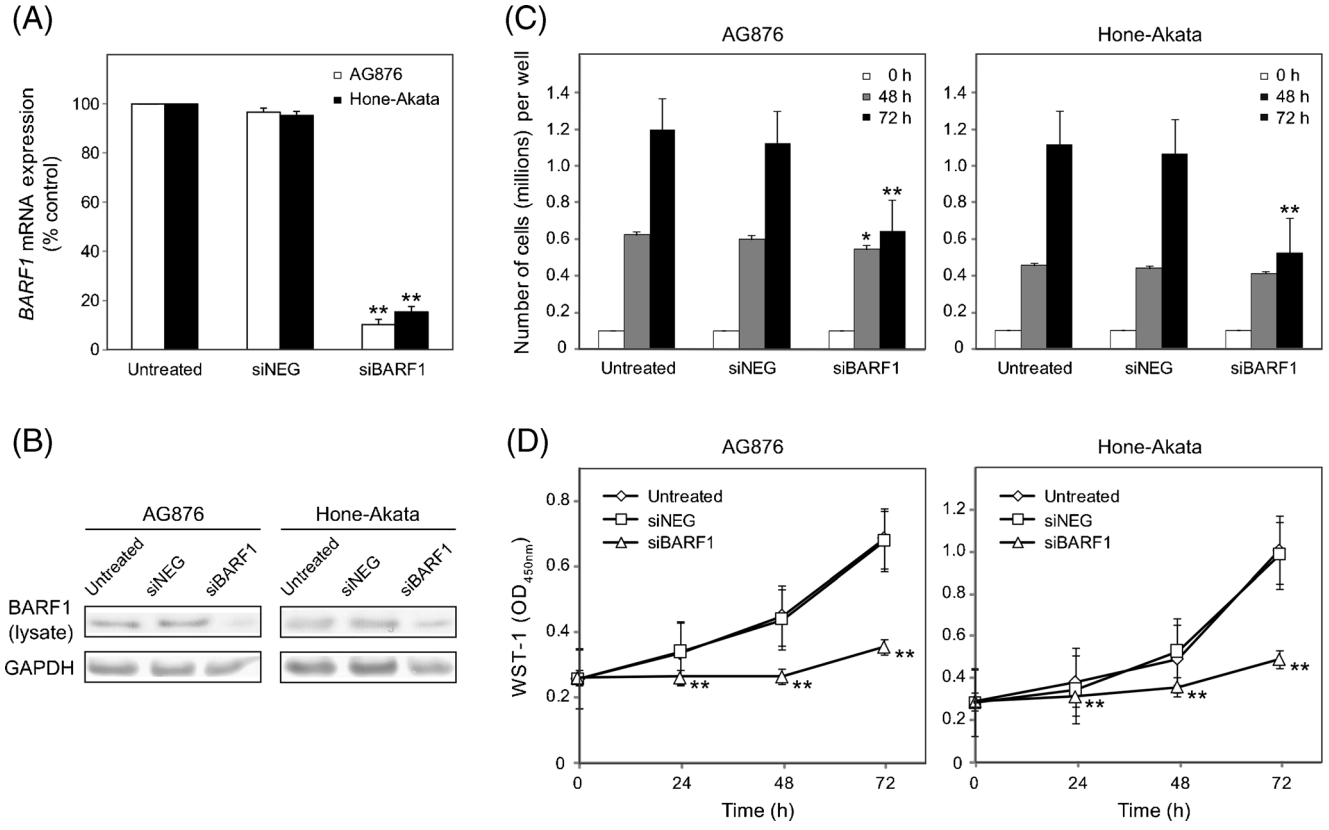

Figure 1. siRNA-mediated BARF1 down-regulation inhibits cell proliferation in AG876 and Hone-Akata cells. (**A**) qRT-PCR analysis of BARF1 expression in AG876 and Hone-Akata cells 72 h after transfection with siNEG and siBARF1. (**B**) Immunoblot analysis of BARF1 protein expression in control and siBARF1-transfected AG876 and Hone-Akata cells. GAPDH was used as loading control. (**C**) Number of viable AG876 and Hone-Akata cells determined using the trypan blue exclusion method. (**D**) WST-1 analysis of the growth of AG876 and Hone-Akata cells after transfection with siNEG and siBARF1. Representative results from three independent experiments are shown as mean±SD (*p<0.05, **p<0.001, significant difference from untreated and siNEG-treated controls).

cells when compared with the controls. At any indicated time point, no obvious antiproliferative effect was exhibited in control cells (figure 1D). Similar antiproliferative effects were exhibited using siBARF1-2 (supplementary figure 1C–D). These results indicate that cell proliferation is inhibited in BARF1-silenced AG876 and Hone-Akata cells.

3.3 *BARF1 down-regulation induces apoptosis-mediated cell death*

Due to the growth inhibitory effects of BARF1 silencing in EBV-positive cancer cells, we next examined the induction of cell death. We examined the apoptosis mediated cell death by flow cytometry analysis using the Annexin V-FITC/PI double fluorescence staining. Simultaneous staining of FITC-conjugated annexin-V with PI discerns early apoptotic cells (annexin-V positive, PI negative) from late apoptotic/dead cells (annexin-V positive, PI positive). BARF1 silencing significantly increased the apoptotic cell population in both AG876 and Hone-Akata cells when compared with untreated and siNEG-treated controls. In AG876 cells, the percentage of early and late apoptotic cell population increased to 37% and 14% respectively following BARF1 depletion. In Hone-Akata cells, BARF1 knockdown increased the early and late apoptotic cell population to 30% and 14% (figure 2A–B). The apoptosis-inducing effect of BARF1 down-regulation was further examined by Western blot analysis for the proteolytic cleavage of PARP, a typical marker for the onset of apoptosis. As shown in figure 2C, the native 116 kDa PARP protein was found to be cleaved to an 89 kDa fragment in BARF1-silenced cells.

3.4 *Down-regulation of BARF1 induces apoptosis by collapsing mitochondrial membrane potential*

The involvement of mitochondria in initiation of apoptosis in cells was evaluated by recording changes in its membrane potential. Analysis of mitochondrial membrane potential

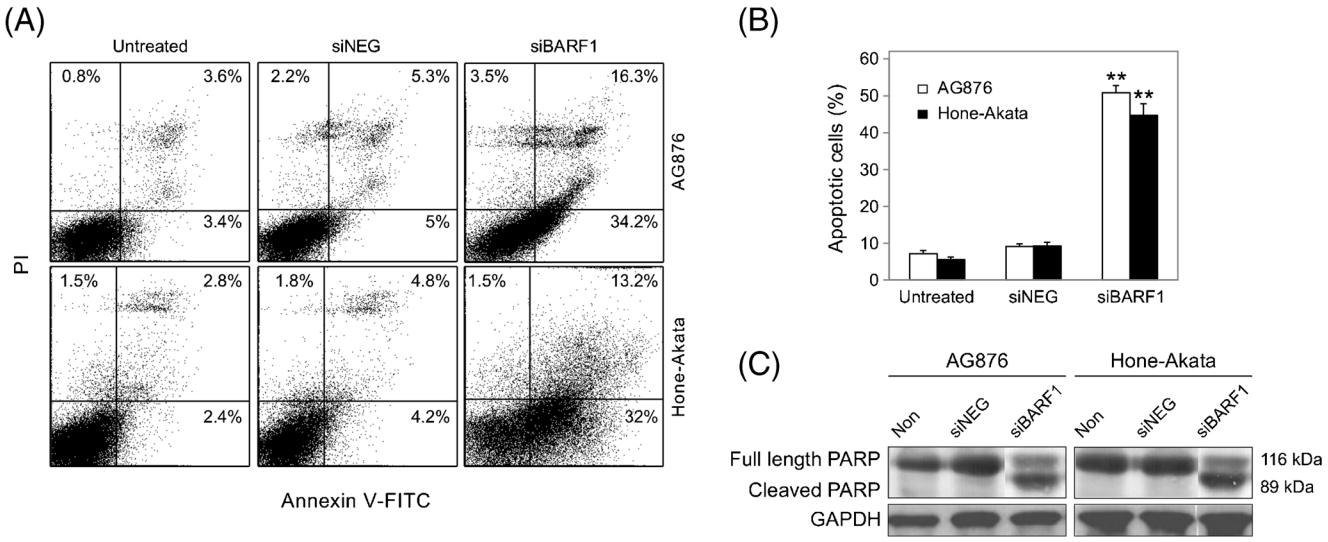

Figure 2. Silencing of BARF1 induces apoptosis-mediated cell death in AG876 and Hone-Akata cells. (**A**) Detection of apoptosis 72 h after transfection with siNEG and siBARF1 using flow cytometry analysis following annexin V-FITC/propidium iodide (PI) dual fluorescence staining. Cells in the lower left quadrant correspond to viable cells, those in the lower right correspond to early apoptotic cells, those in the upper right correspond to late apoptotic cells and those in the upper left correspond to secondary necrotic cells. (**B**) Histograms represent the percentage of apoptotic cells (annexin V-FITC-positive) in control (untreated and siNEG-treated) and siBARF1-transfected cells. Representative data from three independent experiments are shown. Values are mean±SD (**p<0.001, significant difference from untreated and siNEG-treated controls). (**C**) Immunoblot shows degradation of PARP from its 116 kDa native form to the 86 kDa cleaved form, confirming the apoptosis-mediated cell death. GAPDH was used as loading control. The experiments were repeated three times and representative blots are shown.

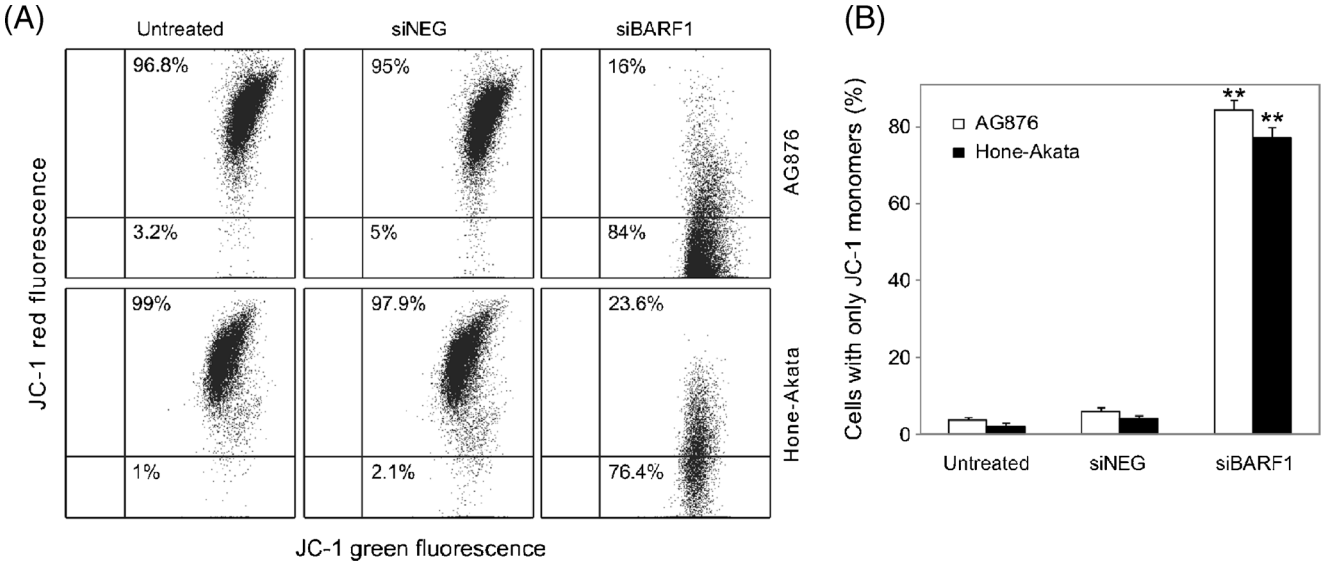

Figure 3. Depletion of BARF1 induces depolarization of MMP in AG876 and Hone-Akata cells. MMP was determined by flow cytometry after staining the control and siBARF1-treated cells with JC-1 fluorescent dye. (**A**) Dot plots show the MMP of cells. In live cells, JC-1 forms red aggregates in mitochondria and exists as green monomers in the cytosol (high MMP). In apoptotic cells, JC-1 exists as green monomers (low MMP). (**B**) Histograms represent the percentage of cells with only JC-1 monomers indicating apoptotic cells with depolarized MMP. The experiments were repeated three times and representative data are shown. Values are mean±SD (**p<0.001, significant difference from untreated and siNEG-treated controls).

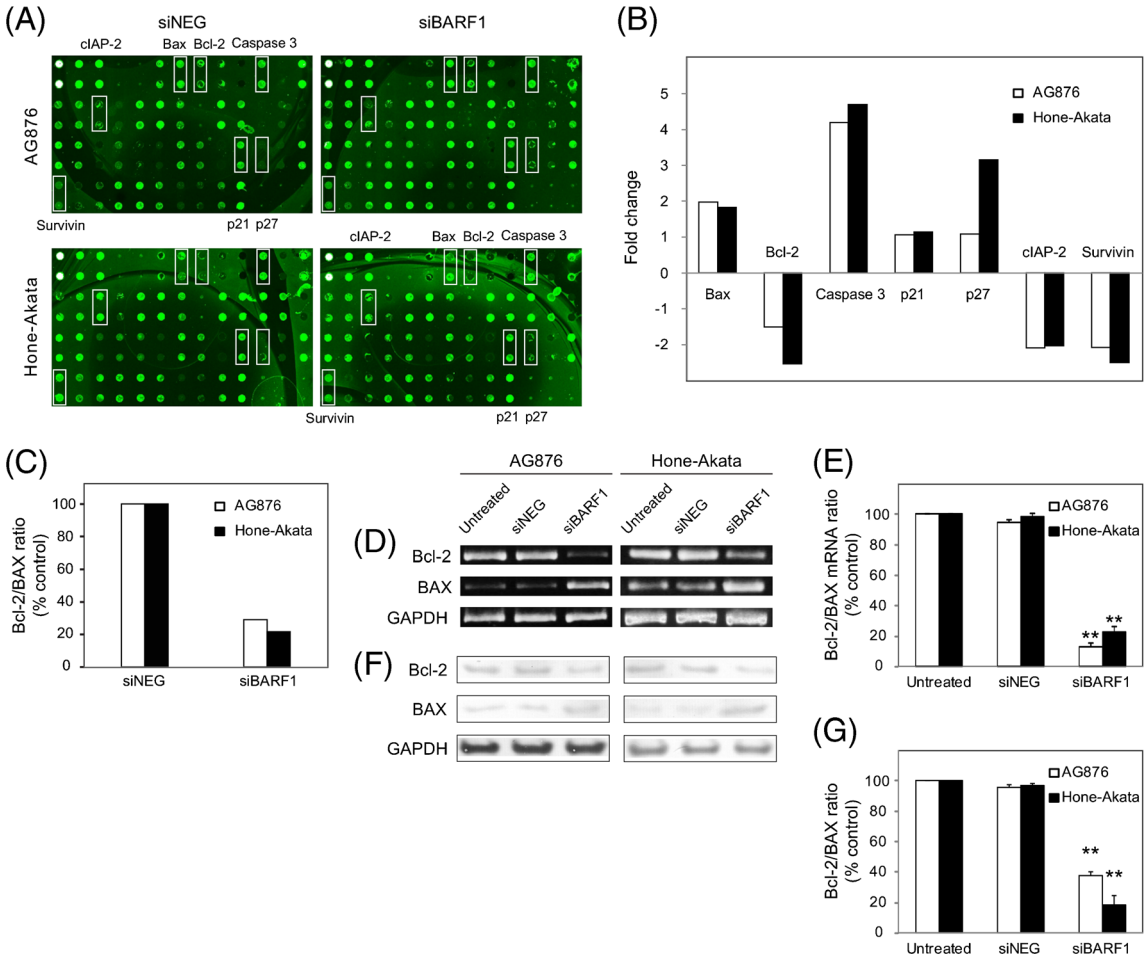

Figure 4. BARF1 down-regulation alters the expression of apoptotic molecules in AG876 and Hone-Akata cells. (**A**) Expression of pro- and anti- apoptotic proteins in AG876 and Hone-Akata cells after transfection with siNEG and siBARF1, analysed using human apoptosis antibody arrays. (**B**) Histograms represent the fold change of apoptotic proteins derived from the fluorescence signal intensities of the arrays. (**C**) Bcl-2/BAX ratio of control and siBARF1-transfected cells based on the fluorescence signal intensities of the apoptosis antibody array. (**D**) Semi-quantitative RT-PCR analysis of Bcl-2 and BAX mRNA expression in control and siBARF1-transfected AG876 and Hone-Akata cells. (**E**) Bcl-2/BAX mRNA ratio analysed by densitometry. (**F**) Immunoblot analysis of Bcl-2 and BAX protein expression in control and siBARF1-transfected AG876 and Hone-Akata cells. GAPDH was used as loading control. (**G**) Bcl-2/BAX protein ratio analysed by densitometry. Representative data from three independent experiments are shown as mean±SD ($^{**}p<0.001$, significant difference from untreated and siNEG-treated controls).

($\Delta\Psi m$) by flow cytometry was done using the APO LOGIX JC-1 Mitochondrial Membrane Potential Assay Kit. The cationic dye (JC-1) forms red aggregates in mitochondria and exists as green monomers in the cytosol of live, non-apoptotic cells. Upon collapse of the mitochondrial membrane potential (MMP) in apoptotic cells, JC-1 remains in the cytoplasm as green monomers. Figure 3A shows that treatment of AG876 and Hone-Akata with siBARF1 resulted in a significant decrease of the red aggregates of JC-1, indicating loss of mitochondrial membrane potential. Transfection with siBARF1 increased the percentage of cells with only JC-1 monomers (apoptotic cells) to 84% and 77% in AG876 and Hone-Akata cells respectively when compared with controls (figure 3B). Knockdown of BARF1 collapsed the mitochondrial membrane potential of EBV-positive tumour cells significantly, confirming the induction of apoptosis in these cells.

3.5 *BARF1 silencing up-regulates the expression of pro-apoptotic proteins and down-regulates the expression of anti-apoptotic proteins*

To evaluate the expression of apoptosis-related proteins, mock- and siBARF1-transfected AG876 and Hone-Akata

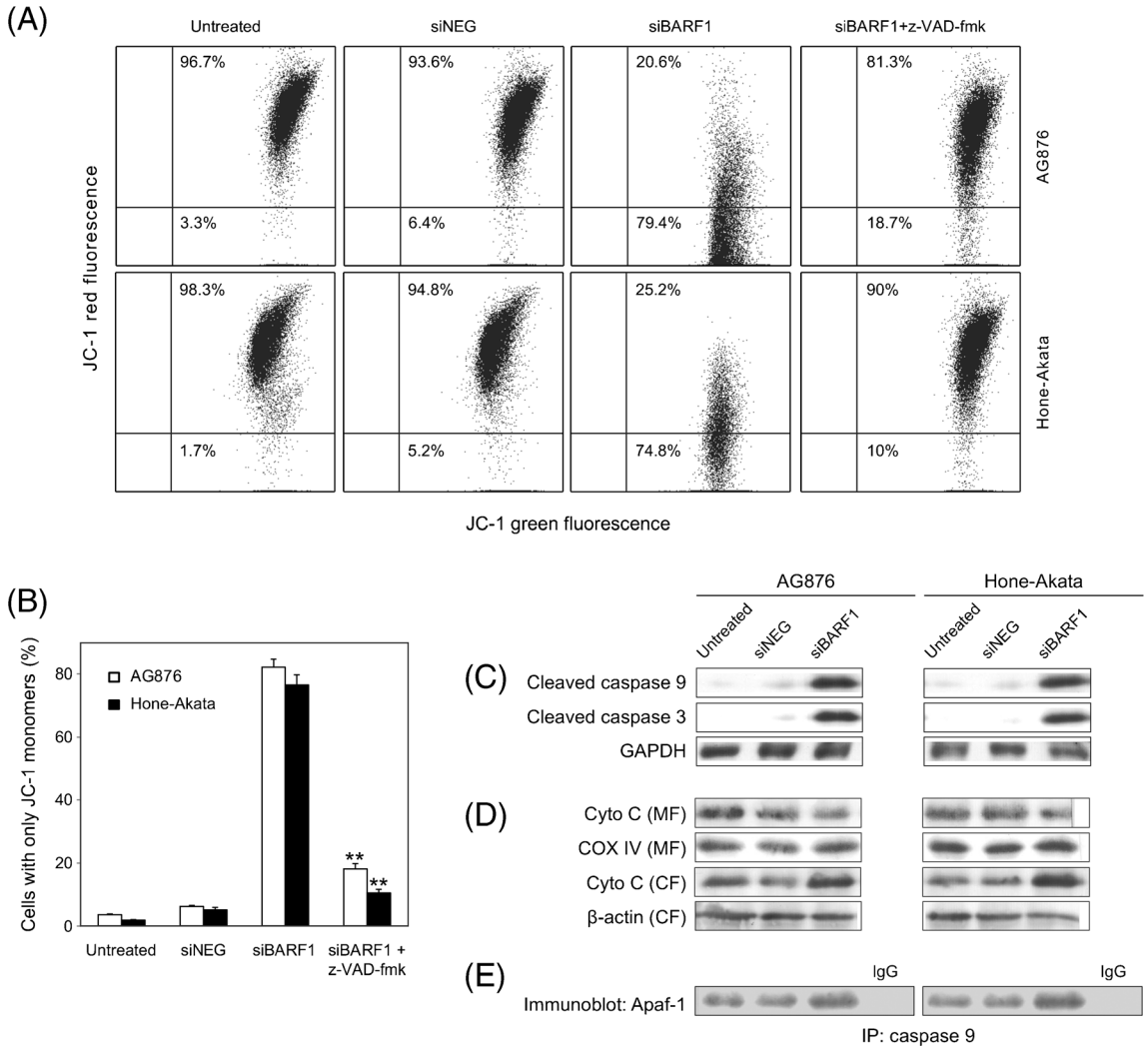

Figure 5. Silencing of BARF1 induces caspase-dependent apoptosis in AG876 and Hone-Akata cells. (**A**) MMP analysis of siBARF1-transfected AG876 and Hone-Akata cells pre-treated with z-VAD-fmk caspase inhibitor by flow cytometry. (**B**) Histograms represent percentage of cells with only JC-1 monomers (apoptotic cells with collapsed MMP). Representative data from three independent experiments are shown as mean±SD (**p<0.001, significant difference from siBARF1-treated cells). (**C**) Western blot analysis of cleaved caspase 9 and cleaved caspase 3 in control and siBARF1-treated cells. GAPDH was used as the loading control. (**D**) Immunoblot for cytochrome c level in mitochondrial fractions (MF) and cytoplasmic fractions (CF). For loading control, cytochrome oxidase IV was used for MF, β-actin was used for CF. (**E**) Immunoprecipitation for Apaf-1 from cell lysates. Cell lysates were immunoprecipitated with anti-caspase 9 antibody and immunoblotted for Apaf-1. Normal rabbit IgG was added to cell lysates as negative control. Immunoblots are representative of three experiments.

cell lysates were analysed using RayBio Human Apoptosis Antibody Array G Series. Antibody array analysis indicated that expression of BAX, caspase 3, p21, and p27 increased while expression of Bcl-2, cIAP-2, survivin decreased in both AG876 and Hone-Akata cells (figures 4A–B). Quantification of protein signals from the array revealed that BAX increased 2-fold in AG876 and 1.8-fold and Hone-Akata cells while Bcl-2 decreased 1.5-fold and 2.5-fold in AG876 and Hone-Akata cells respectively (figure 4B). In siBARF1-transfected cells, Bcl-2/BAX ratio decreased by 71% in AG876 and by 79% in Hone-Akata cells as compared to controls (figure 4C). To ascertain if the decreased Bcl-2 expression and increased BAX expression were caused by gene transcription, we examined the transcript levels of Bcl-2 and BAX using semi-quantitative RT-PCR. The results revealed that expression of Bcl-2 mRNA was decreased by siBARF1 in both AG876 and Hone-Akata cells (figure 4D). Quantification by densitometry showed that the Bcl-2/BAX ratio at the mRNA level decreased

significantly by 87% in AG876 and 78% in Hone-Akata with siBARF1 treatment as compared to the controls (figure 4E). To confirm these results, we checked the expression of Bcl-2 and BAX using western blot analysis. The results revealed that expression of Bcl-2 was decreased whereas BAX expression was increased in BARF1-silenced AG876 and Hone-Akata cells (figure 4F). Quantification by densitometry showed that with siBARF1 treatment, the Bcl-2/BAX ratio at the protein level decreased significantly by 63% in AG876 and 82% in Hone-Akata as compared to the controls (figure 4G).

3.6 *Down-regulation of BARF1 induces caspase-dependent apoptosis*

To investigate the involvement of caspases, we used a broader caspase inhibitor, z-VAD-fmk to examine its ability to prevent apoptosis caused by BARF1 silencing. Analysis of mitochondrial membrane potential collapse by flow cytometry revealed that pretreatment with the broad caspase inhibitor, z-VAD-fmk at 50 μM rescued the apoptosis in siBARF1-treated cells (figures 5A–B). Pretreatment with z-VAD-fmk followed by siBARF1-transfection decreased the percentage of cells with only JC-1 monomers (apoptotic cells) to 18% and 10% in AG876 and Hone-Akata cells respectively when compared with siBARF1 transfected cells. The above results reveal that siBARF1-induced apoptosis in both AG876 and Hone-Akata cells is caspase-dependent.

3.7 *BARF1 knockdown enhances cytochrome c release from mitochondria into cytosol and formation of apoptosome complex*

To examine the roles of activated caspase 3 and caspase 9 in siBARF1-induced apoptosis, we performed western blot analysis. Figure 5C shows that BARF1 knockdown increased cleavage of caspase 3 and caspase 9 significantly as compared to controls in both AG876 and Hone-Akata cells. Cytochrome c, which is released from the mitochondrial membrane into the cytosol facilitates cleavage of caspases (Brunelle and Letai 2009). Therefore, using western blot analysis we examined the levels of cytochrome c in both mitochondrial and cytosolic fractions. We found that the cytochrome c level in the cytosolic fractions of siBARF1-depleted cells was significantly increased as compared to control cells whereas decreased cytochrome c level in the mitochondrial fractions was detected (figure 5D). Cytochrome c is released into the cytosol and binds to the cytosolic apoptotic protease-activating factor (Apaf-1) together with caspase 9 to form the apoptosome (Hajra and Liu, 2004). We performed immunoprecipitation of caspase 9 with anti-caspase 9 followed by western blot detection with anti-Apaf 1 to check the formation of apoptosome complex in BARF1-silenced AG876 and Hone-Akata cells. Our results revealed that Apaf-1 was significantly immunoprecipitated with caspase 9 in BARF1-transfected cells as compared to controls (figure 5E).

4. Discussion

The Epstein-Barr virus-encoded BARF1 is expressed in NPC, EBV-associated GC carcinoma, B cell lymphoma as well as in nasal NK/T-cell lymphoma and is proposed to function as an oncogene (Decaussin *et al*. 2000; Zur Hausen *et al*. 2000; Xue *et al*. 2002; Seto *et al.* 2005; Zhang *et al*. 2006). Although BARF1 is able to induce malignant transformation in rodent cells and human B cell lines (Wei *et al*. 1994; Wei *et al*. 1997) immortalization can only be achieved in primary monkey epithelial cells (Wei *et al*. 1997). Interestingly, in this EBV-induced immortalization, BARF1 expression was detected but LMP1 was absent (Danve *et al*. 2001). Previous studies have suggested that the secreted BARF1 plays a role in promoting cell growth (Wei *et al*. 1997; Sakka *et al*. 2013) as well as in providing protection against apoptosis through an increased Bcl-2 to BAX ratio (Wang *et al*. 2006). However, its anti-apoptotic mechanism remains unclear. RNAi has been used extensively to explore molecular mechanisms of gene functions and also employed as treatment in viral diseases (Gitlin *et al*. 2002). In this study, we assessed the effect of RNAi-mediated knockdown of BARF1 related to cell proliferation and apoptosis in EBV-associated malignant cells. Our preliminary experiment confirmed that AG876 and Hone-Akata cell lines express high levels of BARF1 (data not shown). These cell lines were therefore chosen to evaluate the knockdown effect of BARF1-specific siRNAs.

In this study, we have demonstrated that transfection of BARF1 siRNA into AG876 and Hone-Akata cell lines efficiently down-regulated BARF1 mRNA and protein expression. However, we failed to detect the secreted form of BARF1 protein from the concentrated culture media using immunoblot analysis (data not shown). This may be due to the fact that in our small scale experiment, we were only able to perform medium concentration by a maximum of 1000 fold, unlike by 3000- or 6000-fold as published recently by Chang *et al*. (2013). Results from trypan blue exclusion and WST-1 assays revealed that BARF1 knockdown in these cells led to inhibition of cell proliferation. Our findings confirmed the growth-inhibitory effects of BARF1 siRNA reported very recently in EBV-positive gastric carcinoma by Chang *et al.* (Chang *et al*. 2013). Under microscope, cells appeared rounded and growth of cells treated with siBARF1 was inhibited (data not shown), suggesting apoptosis. The externalization of phosphatidylserine (PS) is one of the earliest events in apoptosis (Martin *et al*. 1995). Cleavage of PARP-1 by caspases is a hallmark of apoptosis (Kaufmann *et al*. 1993; Chaitanya *et al*. 2010). Hence, we conducted flow cytometry analysis of PS

externalization using annexin V-FITC as well as PARP cleavage detection to confirm the mode of cell death. Results from these tests indicate that apoptosis was induced in BARF1-silenced AG876 and Hone-Akata cells.

We next aimed to investigate the molecular mechanisms by which apoptosis is mediated in these BARF1-down-regulated cells. The two major routes of apoptosis are the death receptor (extrinsic) pathway and the mitochondrial (intrinsic) pathway. In the latter, mitochondria plays a central role in the commitment of cells to apoptosis (Fulda and Debatin 2006). In response to apoptotic stimuli, loss of mitochondrial membrane potential is required for mitochondrial-mediated apoptosis (Gottlieb *et al*. 2003; Ly *et al*. 2003). In the present study, we have demonstrated that the apoptosis in BARF1-treated cells was accompanied by a collapse in mitochondrial membrane potential.

Bcl-2 family members are critical regulators of the apoptotic pathway. In the mitochondrial-dependent pathway, interaction between mitochondria and the Bcl-2 family members initiates the release of cytochrome c from the mitochondria. The mechanisms that regulate mitochondrial apoptosis involve pro-apoptotic proteins (e.g. BAX, Bak, Bim) and anti-apoptotic proteins (e.g. Bcl-2, Bcl-xL) of the Bcl-2 family (Oltvai *et al*. 1993; Korsmeyer 1999). The ratio of the anti-apoptotic Bcl-2 to the pro-apoptotic BAX provides a major checkpoint in mammalian cell death pathway (Gross *et al*. 1999). Overexpression of apoptosis-preventing Bcl-2 protein contributes to tumorigenesis in many types of cancers and BAX counteracts this apoptosis-inhibiting effect of Bcl-2 (Reed 1996). In this study, we have shown that BARF1 silencing decreased the Bcl-2/BAX ratio. We also noticed the up-regulation of several pro-apoptotic proteins and the down-regulation of anti-apoptotic proteins in cells with BARF1 depletion.

We have demonstrated that pre-treatment with z-VAD-fmk caspase inhibitor rescued the siBARF1-mediated apoptosis in AG876 and Hone-Akata cells. This indicates that apoptosis mediated by BARF1 down-regulation is caspase-dependent. Apoptotic cell death is often mediated by a caspase cascade. Cytochrome c is released from mitochondria following the collapse of mitochondrial membrane potential. In the cytosol, cytochrome c binds to Apaf-1 and caspase 9 to form the apoptosome (Ledgerwood and Morison 2009). Using western blot analysis, we have shown a significant increase in active caspase 3 and active caspase 9 expressions. We have also demonstrated that a significant level of Apaf-1 was immunoprecipitated with caspase 9 in BARF1-silenced cells, indicating the activation of apoptosome complex formation.

Our data shows that siRNA against the proposed viral oncogene BARF1 is proven to be able to efficiently suppress the BARF1 mRNA expression in EBV-positive malignant cells. We show for the first time that siRNA against BARF1 is able to induce apoptosis-mediated cell death in EBV-positive malignant cells. We conclude that the siRNA-mediated BARF1 down-regulation induced caspase-dependent apoptosis via the mitochondrial pathway through modulation of Bcl-2/BAX ratio. However, to fully define the intracellular signalling pathways in BARF1-depleted cells, further studies of changes in protein expression and activities are needed. Future studies will be directed towards investigation of the effects of BARF1 siRNA *in vivo* as well as the value of BARF1 siRNA in treatment of EBV-associated cancers.

Acknowledgements

We thank Dr Middeldorp from the Department of Pathology, VU University Medical Center, for kindly providing the BARF1 antibody. We also thank Dr Ea Chee Kwee from the Institute of Biological Sciences, University of Malaya, for providing reagents in immunoprecipitation experiment, and Mr Lim Chun Shen for figure preparation for this manuscript.

References

Brunelle JK and Letai A 2009 Control of mitochondrial apoptosis by the Bcl-2 family. *J Cell. Sci.* **122** 437–441

Chaitanya GV, Alexander JS and Babu PP 2010 PARP-1 cleavage fragments: Signatures of cell-death proteases in neurodegeneration. *Cell Commun. Signal* **8** 31

Chang MS, Kim DH, Roh JK, Middeldorp JM, Kim YS, Kim S, Han S, Kim CW, *et al*. 2013 Epstein-Barr virus-encoded BARF1 promotes proliferation of gastric carcinoma cells through regulation of NF-κB. *J. Virol.* **87** 10515–10523

Danve C, Decaussin G, Busson P and Ooka T 2001 Growth transformation of primary epithelial cells with a NPC-derived Epstein–Barr virus strain. *Virology* **288** 223–235

De Turenne-Tessier M, Jolicoeur P, Middeldorp JM and Ooka T 2005 Expression and analysis of the Epstein-Barr virus BARF1-encoded protein from a tetracycline-regulatable adenovirus system. *Virus res.* **109** 9–18

Decaussin G, Sbih-Lammali F, de Turenne-Tessier M, Bouguermouh A and Ooka T 2000 Expression of BARF1 gene encoded by Epstein-Barr virus in nasopharyngeal carcinoma biopsies. *Cancer Res.* **60** 5584–5588

Fiorini S and Ooka T 2008 Secretion of Epstein-Barr virus-encoded BARF1 oncoprotein from latently infected B cells. *Virol. J.* **5** 70

Fulda S and Debatin KM 2006 Extrinsic versus intrinsic apoptosis pathways in anticancer chemotherapy. *Oncogene* **25** 4798–4811

Gitlin L, Karelsky S and Andino R 2002 Short interfering RNA confers intracellular antiviral immunity in human cells. *Nature* **418** 430–434

Glaser R, Zhang HY, Yao KT, Zhu HC and Wang FX 1989 Two epithelial tumor cell lines (HNE-1 and HONE-1) latently infected with Epstein-Barr virus that were derived from nasopharyngeal carcinomas. *Proc. Natl. Acad. of Sci. USA* **86** 9524–9528

Gottlieb E, Armour SM, Harris MH and Thompson CB 2003 Mitochondrial membrane potential regulates matrix configuration and cytochrome c release during apoptosis. *Cell Death Differ.* **10** 709–717

Gross A, McDonnell JM and Korsmeyer SJ 1999 BCL-2 family members and the mitochondria in apoptosis. *Genes Dev.* **13** 1899–1911

Hajra KM and Liu JR 2004 Apoptosome dysfunction in human cancer. *Apoptosis Int. J. Program. Cell Death* **9** 691–704

Hoebe EK, Hutajulu SH, van Beek J, Stevens SJ, Paramita DK, *et al*. 2011 Purified hexameric Epstein-Barr virus-encoded BARF1 protein for measuring anti-BARF1 antibody responses in nasopharyngeal carcinoma patients. *Clin. Vaccine Immunol. CVI* **18** 298–304

Hoebe EK, Le Large TYS, Tarbouriech N, Oosterhoff D, De Gruijl TD, *et al*. 2012a Epstein-Barr Virus-encoded BARF1 protein is a decoy receptor for macrophage colony stimulating factor and interferes with macrophage differentiation and activation. *Viral Immunol.* **25** 461–470

Hoebe EK, Wille C, Hopmans ES, Robinson AR, Middeldorp JM, *et al*. 2012b Epstein-Barr virus transcription activator R upregulates BARF1 expression by direct binding to its promoter, independent of methylation. *J. Virol.* **86** 11322–11332

Houali K, Wang X, Shimizu Y, Djennaoui D, Nicholls J, *et al*. 2007 A new diagnostic marker for secreted Epstein-Barr virus–encoded LMP1 and BARF1 oncoproteins in the serum and saliva of patients with nasopharyngeal carcinoma. *Clin. Cancer Res.* **13** 4993–5000

Jiang R, Cabras G, Sheng W, Zeng Y and Ooka T 2009 Synergism of BARF1 with Ras induces malignant transformation in primary primate epithelial cells and human nasopharyngeal epithelial cells. *Neoplasia N Y N* **11** 964–973

Kaufmann SH, Desnoyers S, Ottaviano Y, Davidson NE and Poirier GG 1993 Specific proteolytic cleavage of Poly(ADP-Ribose) polymerase: an early marker of chemotherapy-induced apoptosis. *Cancer Res.* **53** 3976–3985

Korsmeyer SJ 1999 BCL-2 gene family and the regulation of programmed cell death. *Cancer Res.* **59** 1693s–1700s

Ledgerwood EC and Morison IM 2009 Targeting the apoptosome for cancer therapy. *Clin. Cancer Res.* **15** 420–424

Ly JD, Grubb DR and Lawen A 2003 The mitochondrial membrane potential (deltapsi(m)) in apoptosis; an update. *Apoptosis Int. J. Program. Cell Death* **8** 115–128

Martin SJ, Reutelingsperger CP, McGahon AJ, Rader JA, Schie RC, *et al*. 1995 Early redistribution of plasma membrane phosphatidylserine is a general feature of apoptosis regardless of the initiating stimulus: inhibition by overexpression of Bcl-2 and Abl. *J. Exp. Med.* **182** 1545–1556

Oltvai ZN, Milliman CL and Korsmeyer SJ 1993 Bcl-2 heterodimerizes in vivo with a conserved homolog, Bax, that accelerates programmed cell death. *Cell* **74** 609–619

Reed JC 1996 Balancing cell life and death: bax, apoptosis, and breast cancer. *J. Clin. Invest.* **97** 2403–2404

Sakka E, Zur Hausen A, Houali K, Liu H, Fiorini S, *et al*. 2013 Cellular localization of BARF1 oncoprotein and its cell stimulating activity in human epithelial cell. *Virus Res.* **174** 8–17

Sall A, Caserta S, Jolicoeur P, Franqueville L, de Turenne-Tessier M, *et al*. 2004 Mitogenic activity of Epstein-Barr virus-encoded BARF1 protein. *Oncogene* **23** 4938–4944

Seto E, Yang L, Middeldorp J, Sheen TS, Chen JY, *et al*. 2005 Epstein–Barr Virus (EBV)-encoded BARF1 gene is expressed in nasopharyngeal carcinoma and EBV-associated gastric carcinoma tissues in the absence of lytic gene expression. *J Med. Virol.* **76** 82–88

Seto E, Ooka T, Middeldorp J and Takada K 2008 Reconstitution of nasopharyngeal carcinoma-type EBV infection induces tumorigenicity. *Cancer Res.* **68** 1030–1036

Sheng W, Decaussin G, Sumner S and Ooka T 2001 N-terminal domain of BARF1 gene encoded by Epstein-Barr virus is essential for malignant transformation of rodent fibroblasts and activation of BCL-2. *Oncogene* **20** 1176–1185

Sheng W, Decaussin G, Ligout A, Takada K and Ooka T 2003 Malignant transformation of Epstein-Barr virus-negative Akata cells by introduction of the BARF1 gene carried by Epstein-Barr virus. *J. Virol.* **77** 3859–3865

Tanner JE, Wei MX, Alfieri C, Ahmad A, Taylor P, *et al*. 1997 Antibody and antibody-dependent cellular cytotoxicity responses against the BamHI A Rightward Open-Reading Frame-1 Protein of Epstein-Barr virus (EBV) in EBV-associated disorders. *J. Infect. Dis.* **175** 38–46

Wang Q, Tsao SW, Ooka T, Nicholls JM, Cheung HW, *et al*. 2006 Anti-apoptotic role of BARF1 in gastric cancer cells. *Cancer Lett.* **238** 90–103

Wei MX, Turenne-Tessier M, Decaussin G, Benet G and Ooka T 1997 Establishment of a monkey kidney epithelial cell line with the BARF1 open reading frame from Epstein-Barr virus. *Oncogene* **14** 3073–3081

Wei MX and Ooka T 1989 A transforming function of the BARF1 gene encoded by Epstein-Barr virus. *EMBO J.* **8** 2897–2903

Wei MX, Moulin JC, Decaussin G, Berger F and Ooka T 1994 Expression and tumorigenicity of the Epstein-Barr virus BARF1 gene in human Louckes B-lymphocyte cell line. *Cancer Res.* **54** 1843–1848

Xue S, Labrecque LG, Lu QL, Ong SK, Lampert IA, *et al*. 2002 Promiscuous expression of Epstein-Barr virus genes in Burkitt's lymphoma from the central African country Malawi. *Int. J. Cancer* **99** 635–643

Zhang Y, Ohyashiki JH, Takaku T, Shimizu N and Ohyashiki K 2006 Transcriptional profiling of Epstein–Barr virus (EBV) genes and host cellular genes in nasal NK/T-cell lymphoma and chronic active EBV infection. *Br. J. Cancer* **94** 599–608

Zur Hausen A, Brink AATP, Craanen ME, Middeldorp JM, Meijer CJLM, *et al*. 2000 Unique transcription pattern of Epstein-Barr virus (EBV) in EBV-carrying gastric adenocarcinomas: Expression of the transforming BARF1 gene. *Cancer Res.* **60** 2745–2748

MS received 02 September 2014; accepted 07 January 2015

Corresponding editor: Seyed E Hasnain